Remigration-trajectory time-migration velocity analysis in regions with strong velocity variations

H. B. Santos* (CEP/UNICAMP & INCT-GP), T. A. Coimbra (IMECC-UNICAMP & INCT-GP), J. Schleicher (IMECC/UNICAMP & INCT-GP) and A. Novais (IMECC/UNICAMP & INCT-GP)

Abstract

Remigration trajectories describe the position of an image point in the image domain for different source-receiver offsets as a function of the migration velocity. They can be used for prestack time-migration velocity analysis by means of determining kinematic migration parameters, which in turn, allow to locally correct the velocity model. The main advantage of this technique is that it takes the reflection-point displacement in the midpoint direction into account, thus allowing for a moveout correction for a single reflection point at all offsets of a common image gather (CIG). We have tested the feasibility of the method on synthetic data from three simple models and the Marmousoft data. Our tests show that the proposed tool increases the velocity-model resolution and provides a plausible time-migrated image, even in regions with strong velocity variations. The most effort was spent on the event picking, which is critical to the method.

Introduction

Remigration, also known as residual migration or velocity continuation, can be seen as a process to construct a seismic image for a refined velocity model from another one already available from a previous migration for a different velocity model (Hubral et al., 1996; Tygel et al., 1996). Velocity continuation can be also used on migrated diffractions (Sava et al., 2005; Fomel et al., 2007; Novais et al., 2008) for MVA. Based on velocity continuation, Coimbra et al. (2013b) recently introduced a process of extracting velocity updates for depth migration from the moveout of incorrectly migrated diffraction events by tracing remigration trajectories to their focus point in post-stack migrated images, and Coimbra et al. (2013a) extended their work to the prestack case. This technique makes use of local-slope information extracted from the data with the help of trail stacks. Coimbra et al. (2014) modified this remigration-trajectory MVA method to make it suitable for an application to time-migration of reflection events in prestack data, presenting an improved derivation of the time-remigration trajectories. In this work, we present an improved derivation of the method's theory as compared to Coimbra et al. (2014), detail the model-building algorithm, and report on numerical tests of the method applied to synthetic data from three gradient models and to the Marmousoft data. These additional tests confirm the potential of the method to produce plausible velocity-model updates in regions with strong velocity variations.

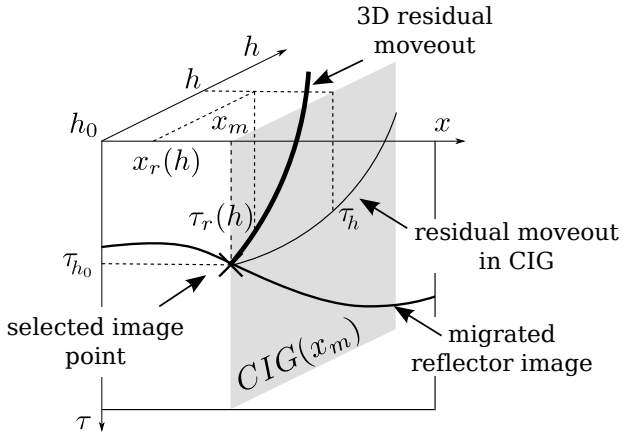

Figure 1: The residual moveout of a dipping reflector in a single CIG at x_m after migration with a wrong velocity is described by curve τ_h (fine line). However, the image of a unique reflection point moves out of the CIG through the whole migrated data volume along a 3D moveout curve $\tau_r(h)$ (bold solid line). This curve can be approximated from information found at point (h_0, x_m, τ_{h_0}). For details, see text.

Remigration Trajectory

The residual moveout of a point on the migrated image of a dipping reflector as a function of half-offset is a three-dimensional curve through the prestack-migrated data volume (see Figure 1). A remigration trajectory describes the position of a point on this moveout curve as a function of migration velocity, considering not only the half-offset, but also the variation of the reflection-point displacement in the midpoint direction (see Figure 2).

The method of Coimbra et al. (2013c, 2014) and Santos et al. (2014) consists of analyzing the local slope of selected key reflections and determining the velocity value for which an approximate residual-moveout (RMO) expression is minimized. The advantage of this procedure over conventional MVA methods is that the RMO expression follows the events outside a fixed CIG.

Application to constant-gradient models

We applied the method to three constant-gradient models that can be thought of as representing subregions of a larger model. To verify the feasibility of our method,

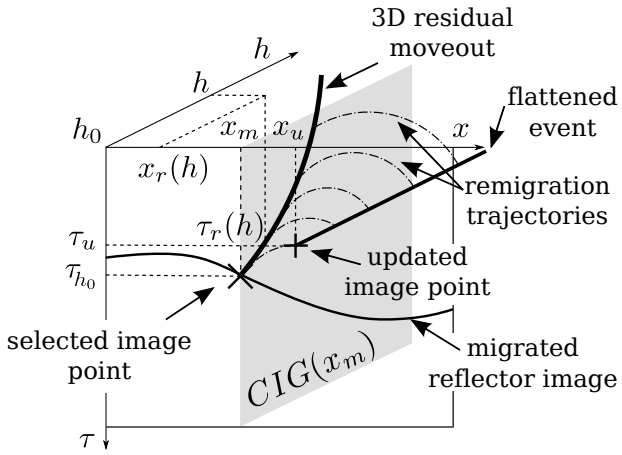

Figure 2: Remigration trajectories (dash-dotted lines) for selected points on the 3D moveout curve (bold solid line) of an incorrectly migrated reflector point (x_m, τ_{h_0}). Also shown is the flattened position of the event at (x_u, τ_u).

which was derived under the assumption of constant average velocities, in more realistic situations, we chose rather strong velocity gradients in the vertical, horizontal, and diagonal directions. The true velocity models are given by $v(z) = 2000 + 0.5z$ m/s, $v(x) = 2000 + 0.5x$ m/s and $v(x,z) = 2000 + 0.5x + 0.5z$ m/s. All three models contain six interfaces with, from top to bottom, initial depths at the origin of 400 m, 500 m, 600 m, 700 m, 800 m, and 900 m, and dips of 0°, 4.8°, 10°, 15°, 23.6°, 39.5°, respectively. Moreover, they contain seven diffraction points not used for velocity analysis. Their only purpose is the quality control of the extracted velocity models. We generated synthetic data with Kirchhoff modelling using a symmetric Ricker wavelet with 20 Hz peak frequency, and contaminated the data with white noise at a level of 5% of the maximum amplitude.

We then applied the present remigration-trajectory MVA method to these data. The first step consisted in a constant-velocity time migration. For these examples, we used an intermediate velocity of $v_0 = 3.0$ km/s.

Figure 3a depicts the true velocity model with reflectors and control diffractors, and Figure 3b shows the time-migrated zero-offset section using a constant migration velocity of 3000 m/s. From this initial migration, we started the remigration-trajectory velocity analysis. To investigate the quality of the result in dependence of the number of points picked, we performed the analysis twice, once with 21 image points and once with 100 image points. Figure 4a shows the 21 image points picked in the first run (black crosses) together with their updated positions (pink plusses) superimposed over the obtained updated velocity model after one iteration. This model results from a B-splines interpolation of the updated velocities at the 21 updated image-point locations. Figure 4b shows the corresponding time-migrated stacked section. In the velocity model, we recognize some undulations, indicating that the velocity estimate is better at the chosen image points than in their vicinity. Nonetheless, the control diffractors in the image are reasonably focused and the reflectors only slightly curved. This indicates that the model in Figure 4a already is an acceptable time-migration

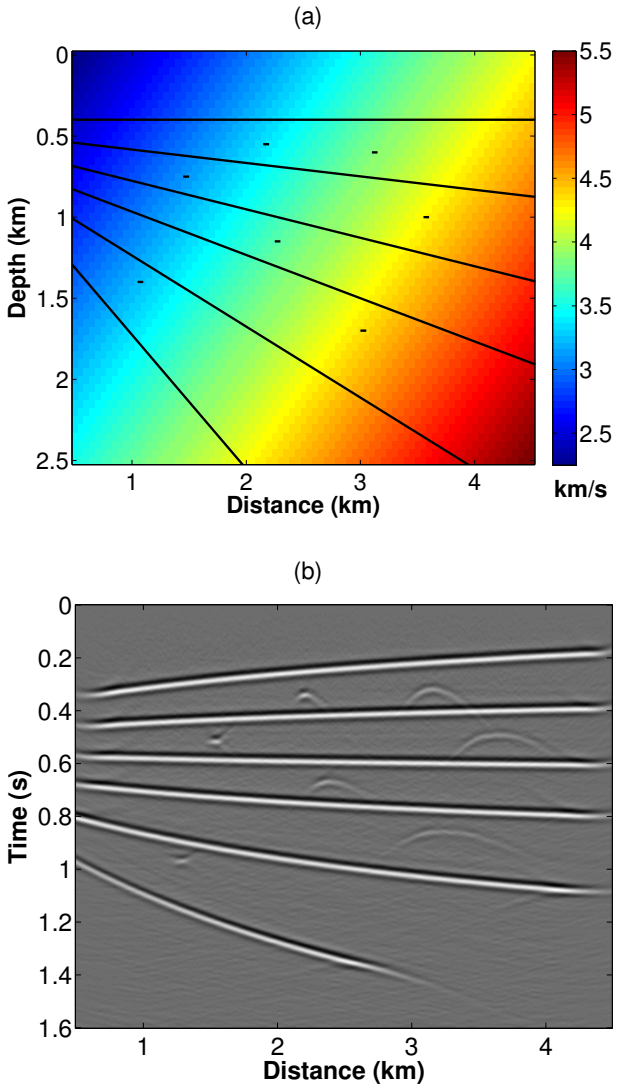

Figure 3: Diagonal-gradient model: (a) Velocity model with reflectors and control diffractors. (b) Time-migrated image using $v_0 = 3.0$ km/s.

velocity model. Next, we applied two passes of moving-average smoothing with a 1 km × 0.4 s (100 by 100 points) window. The idea is to carry the velocity information at the chosen image points over to their vicinities where no updated velocity values are available. Figures 4c and d show the corresponding model and image. While the model has improved and resembles the true model of Figure 3a more closely, the time-migrated image of Figure 4d is almost identical to that of Figure 4b. Figure 4e shows the 100 image points picked in the second test (black crosses), also together with their updated positions (pink plusses) and superimposed over the obtained updated velocity model after one iteration. Again, Figure 4f shows the corresponding time-migrated stacked section. In comparison to Figure 4a, we observe that the velocity undulations in Figure 4e are reduced in amplitude and wavelength. The migrated image in Figure 4f has slightly improved as compared to Figure 4b, particularly regarding the positioning of the deepest reflector and the focusing of the deepest diffractor. Moving-average smoothing further improves the model (Figure 4g), but again has little effect

on the resulting image (Figure 4h).

Similar conclusions can be drawn from the corresponding experiments with the horizontal and vertical gradients. These tests demonstrate that even in the presence of a strong velocity gradient, the method is capable of extracting meaningful time-migration velocity models using a not too large number of image points where reflector images can be picked in the incorrectly migrated image.

Application to the Marmousoft data

Encouraged by these results, we set out for a more realistic test. We applied the described MVA technique to the Marmousoft data (Billette et al., 2003). These data were constructed by Born modeling in a smoothed version of the Marmousi model. We chose this model so as to analyze the behaviour of our MVA method in a complex sedimentary geology. We did not expect the method to work in the central part of the model because of the limits of time migration. The Marmousoft data contain traces at every 25 meters with a sampling rate of 4 ms. Figure 5a shows a short-offset section with a total source-receiver offset of 100 m. We used 96 common-offset sections with source-receiver offsets between 100 m and 2475 m to apply the remigration-trajectory MVA method. For the first migration, we chose $v_0 = 2.0$ km/s. Figure 5b depicts the migrated image obtained from the short-offset data of Figure 5a. The migration aperture used was 241 traces. Next, we picked 70 points on some of the most prominent migrated events in the image of Figure 5b. At the positions of these picks, we extracted local slopes in the migrated common-offset section and then minimized the residual moveouts along the remigration trajectories as described above. Figure 5c shows the locations of our picks (black crosses) and their corrected positions after velocity updating (pink plusses) overlain on the resulting updated velocity model. As before, we used B-splines to interpolate the velocity model in the complete region. We recognize that the updated velocity model leads to an improved migrated image (Figure 5d), particularly regarding the upper parts of the fault lines and the reflectors in the sedimentary regions on both sides of the model. To eliminate the unrealistic oscillations in the velocity model of Figure 5c, we smoothed it by two passes of a moving average with a 2.5 km$\times$0.4 s (100 by 100 points) window (see Figure 5e). Although the velocity models of Figures 5c and e are rather different, the corresponding migrated images (Figures 5d and f) are quite similar, indicating that both velocity models are equivalent regarding the final time-migration result. These results are in agreement with those produced by common-image gather image-wave propagation and double multi-stack migration (see Santos et al. (2013a) and Santos et al. (2013b) for a parameterization discussion). For further evaluation of the model quality, a time-to-depth conversion will be necessary to compare the attainable model quality as well as to check its application as an initial model for tomographic or depth MVA methods.

Conclusions

We have investigated an MVA tool that uses the estimation of local kinematic attributes of selected events in seismic data to update the velocity model and improve the positioning of key reflectors. We have provided additional numerical tests with strong lateral velocity variation. In these tests, the method led to acceptable time-migration velocity models in a single iterations, even if the starting model was simply a constant velocity. Also the sedimentary shallow part of the Marmousoft model was satisfactorily resolved in one iterations. Tests with different numbers of picked event points demonstrated that the number of points does not need to be very large. Our results indicated that a step of smoothing the data can be helpful, especially for deeper and/or steeper events.

Acknowledgments

This research was supported by Petrobras and CGG as well as the Brazilian research agencies CNPq, FAPESP, FINEP, and CAPES. The first author (HBS) thanks CGG-Brazil for his fellowship. Additional support for the authors was provided by the sponsors of the *Wave Inversion Technology (WIT) Consortium*. Past WIT Reports are available at www.wit-consortium.de.

References

Billette, F., S. Le Bégat, P. Podvin, and G. Lambaré, 2003, Practical aspects and applications of 2D sterotomography: Geophysics, **68**, 1008–1021.

Coimbra, T. A., J. J. S. de Figueiredo, A. Novais, J. Schleicher, and S. Arashiro, 2013a, Migration velocity analysis using residual diffraction moveout in the pre-stack depth domain: Annual WIT report, **17**, 44–53.

Coimbra, T. A., J. J. S. de Figueiredo, J. Schleicher, A. Novais, and J. Costa, 2013b, Migration velocity analysis using residual diffraction moveout in the poststack depth domain: Geophysics, **78**, S125–S135.

Coimbra, T. A., H. B. Santos, J. Schleicher, and A. Novais, 2013c, Migration velocity analysis using time-remigration trajectory in prestack data: Presented at the Proceedings 13th International Congress of The Brazilian Geophysical Society 2013, SBGf.

———, 2014, Prestack migration velocity analysis using time-remigration trajectories: Presented at the Proceedings 76th EAGE Conference and Exhibition 2014, EAGE Publications BV.

Fomel, S., E. Landa, and M. T. Taner, 2007, Poststack velocity analysis by separation and imaging of seismic diffractions: Geophysics, **72**, U89–U94.

Hubral, P., J. Schleicher, and M. Tygel, 1996, A unified approach to 3-D seismic reflection imaging - Part I: Basic concepts: Geophysics, **61**, 742–758.

Novais, A., J. Costa, and J. Schleicher, 2008, GPR velocity determination by image-wave remigration: Journal of Applied Geophysics, **65**, 65–72.

Santos, H. B., T. A. Coimbra, J. Schleicher, and A. Novais, 2014, Prestack time-migration velocity analysis using remigration trajectories: Geophysics. (Submitted).

Santos, H. B., J. Schleicher, and A. Novais, 2013a, Initial-model construction for MVA techniques: Presented at the Expanded Abstracts, 75th EAGE Conference & Exhibition, EAGE Publications BV.

———, 2013b, Initial-model construction for MVA techniques: Annual WIT report, **17**, 124–135.

Sava, P., B. Biondi, and J. Etgen, 2005, Wave-equation migration velocity analysis by focusing diffractions and reflections: Geophysics, **70**, U19–U27.

Tygel, M., J. Schleicher, and P. Hubral, 1996, A unified approach to 3-D seismic reflection imaging - Part II: Theory: Geophysics, **61**, 759–775.

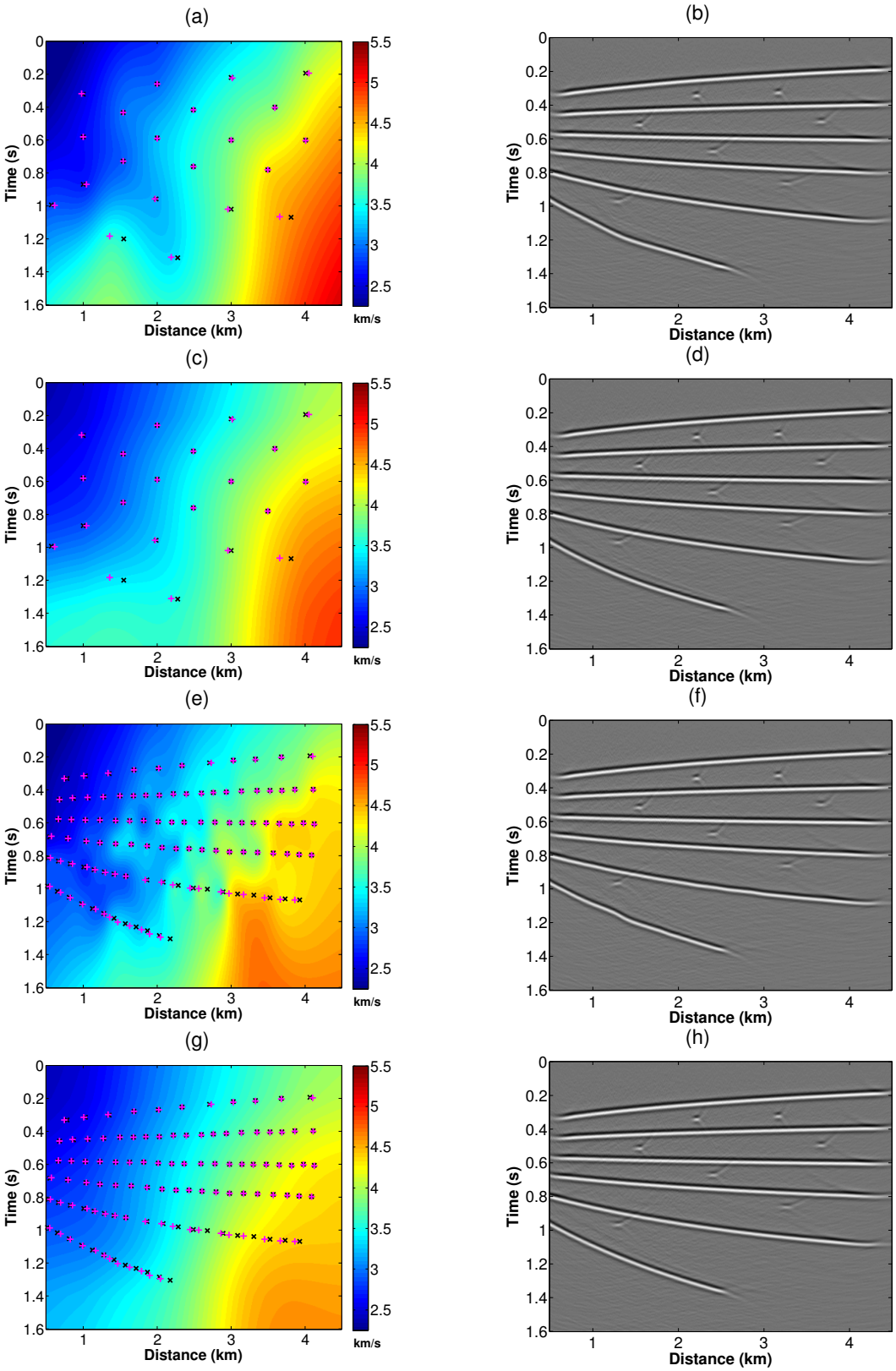

Figure 4: Diagonal-gradient model: (a) Extracted velocity model after one iteration with 21 image points and (b) corresponding final time-migrated image. (c) Extracted velocity model after moving-average smoothing and (d) corresponding final time-migrated image. Also shown in parts (a) and (c) are the picked image points (black crosses) and their updated positions (pink plusses). Results obtained with 100 image points are present from (e) to (h) respectively.

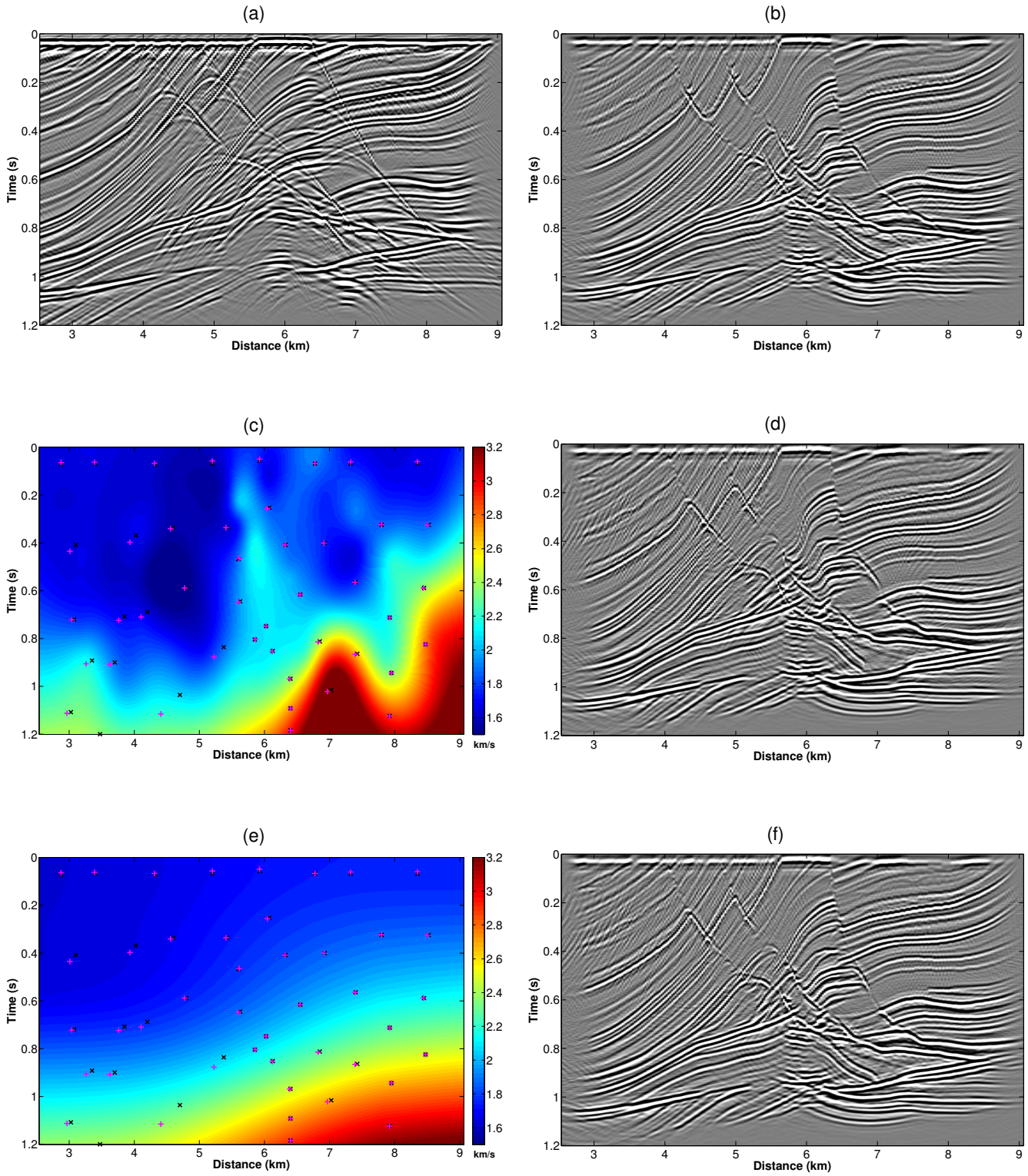

Figure 5: Single iteration of remigration-trajectory MVA on the Marmousoft data. (a) Seismic near-offset section. (b) Time-migrated image of the seismic near-offset section using a constant velocity $v_0 = 2$ km/s and migration aperture equal to 141 traces. (c) Extracted velocity model after one iteration. Also shown are the 70 picked image points (black crosses) and their updated positions (pink plusses). (d) Final time-migrated image by a migration aperture equal to 241 traces. (e) and (f) show the results after moving-average smoothing by two passes with a 2.5 km$\times$0.4 s (100 by 100 points) window.